

Solution properties and characterization of polyisoprenes at a lower critical solution temperature (LCST)

Takouhi Bohossian, Gérard Charlet* and Geneviève Delmas

Chemistry Department, Université du Québec à Montréal, C.P. 8888 Suc. A, Montréal, Canada H3C 3P8

(Received 21 July 1988; revised 16 November 1988; accepted 30 December 1988)

This paper reports two investigations on polyisoprene. One consists of obtaining the molecular weight distribution (MWD) of *cis*-polyisoprene (PIP) standards by a new method using the turbidity at a lower critical solution temperature (LCST). Advantage is taken for this analysis of the fact that the *MW* dependence of the critical temperature is greater for systems with a narrow solubility gap, i.e. for systems whose LCST and upper critical solution temperature (UCST) are not too far apart. Typically, in *n*-pentane, a narrow *MW* standard phase-separates over 25 K. When the solution is heated by temperature increments of 2 K, 15 fractions can be identified, without physical separation. The relative amount of each phase is analysed by turbidity and the average *MW* of the phases by the temperature at which they phase separate. The *MW*s recalculated with two constants for the standards are in excellent agreement with gel permeation chromatography (g.p.c.) data. Possible effects leading to a higher polydispersity found by the LCST are discussed. Application to rubber analysis is feasible. The second investigation consists of reporting and analysing the temperatures of phase separation of medium *MWD cis*- and *trans*-PIP samples in a series of linear and branched alkanes. The occurrence of correlations of molecular orientations (CMO) in the melt, similar to those found from thermodynamic analysis of PE solutions, was considered. *Trans*-PIP has a LCST about 25 K lower than *cis*-PIP in alkanes. Linear solvents are better solvents than branched ones. The low LCSTs (100°C in *n*-pentane) support CMO or order in polyisoprene melt or concentrated solutions.

(Keywords: polyisoprene; lower critical solution temperature; distribution of molecular weight; correlations of molecular orientations)

INTRODUCTION

The general occurrence of a phase separation at high temperature for polymer solutions found about 30 years ago¹ has led to the development of more refined theories of polymer solutions²⁻⁶. The physical and theoretical understanding of the lower critical solution temperature (LCST) permitted the addition of a reason other than the low combinatorial entropy of mixing for the relatively low solubility of polymers: the reduction of free volume of the solvent when mixed with the polymer. However, relatively few studies have been made of the information one can get on the polymer itself from the values of its LCST in different solvents. In this paper, dealing with polyisoprene (PIP), a new method for the characterization of the molecular weight distribution (MWD) based on turbidity at the LCST is presented and an analysis is made of the LCST of *cis*- and *trans*-PIP in a series of alkanes. The second part of the paper is an extension of previous work on the LCST of polyethylene (PE) which supported the idea of correlations of molecular orientations (CMO) in concentrated PE solutions and in the melt⁷.

Narrow solubility gap in macromolecular solutions

Apart from the creation of combinatorial entropy, the dissolution of a small molecule in a solvent is

accompanied by two main contributions, one associated with the change of contacts from the pure components to the solution, the other with the change of free volume during the mixing. If the two components have a large difference in expansion coefficients, as is the case when one of the components is a polymer, the second term is large and leads to a lower critical solution temperature (LCST). If solvent and polymer are chemically similar, this second term is the main contribution to the thermodynamic properties of mixing, at high temperature. When a non-polar polymer is mixed with a polar solvent (or vice versa), the first term is also large, leading to a separation of phase at low temperature or upper critical solution temperature (UCST). If the temperature of a solution is raised, a LCST is likely to occur not too far above the UCST if the solvent is volatile and also chemically different from the polymer. Sometimes, the two effects overlap so much that the solubility gap between the UCST and LCST becomes narrower and narrower. For a given polymer-solvent system, the size of the gap is very sensitive to molecular weight (*MW*). When the *MW* reaches a critical value, the coexistence curves present an hour-glass shape, which reflects total solubility only in dilute or concentrated solutions. Atactic polymers which form a UCST rather than crystallizing from solution at low temperature, such as polystyrene⁸⁻¹¹ polymethylstyrene^{12,13}, polybutadiene¹⁴ and polydimethylsiloxane, have been used to investigate such behaviour and test the theories of solutions²⁻⁶ which

*Present address: Université Laval, Chemistry Department, Québec, Canada, G1K 7P4 and to whom correspondence should be sent

can predict the magnitude of the free volume term or the balance between the contact energy and free volume differences between polymer and solvent. The MW dependence of the UCST and LCST can be predicted and compared with the experimental results⁵. The coexistence curves at the UCST and the LCST are usually mirror images of each other with respect to a median temperature where solubility is a maximum and the free energy interaction parameter χ is at its minimum. Around the median temperature χ varies only very slowly with T , which has an interesting consequence for fractionation: in systems with a narrow miscibility gap, the MW dependence of the phase separation temperature is very pronounced even in the high MW region.

The first aim of this work was to take advantage of this effect by measuring the LCST of five *cis*-polyisoprene standards in a volatile alkane solvent. The MW distribution of these samples, previously characterized by g.p.c., was obtained by a method developed recently on polyethylene¹⁵ and based on measurements of turbidity at a LCST as described below. Furthermore, the results presented here for PIP can find application in the analysis of native rubbers and modified rubbers¹⁶, due to the chemical similarity between the synthetic and natural polymers.

The contribution which raises the χ parameter at low temperature and produces a UCST and a low LCST may not be 'chemical' in nature but may come from structural effects associated with the formation of the solution from the two pure components, the polymer melt and the liquid.

The second aim of this work was to analyse the trends of LCST of *cis*- and *trans*-PIP in series of branched and linear alkanes and to compare the actual values with those obtained for other polyolefins in the same solvents.

LCST AND MOLECULAR WEIGHT DISTRIBUTION

Range of phase separation temperature for narrow MWD samples

Analyses in the literature of cloud-point curves at the UCST, LCST or both have been achieved on narrow MWD samples ($M_w/M_n \approx 1.1$). The characteristic temperature of a system, relevant to M_w and M_w/M_n , is reported with unanimity in the literature as the minimum of $T_0(\phi_2)$, ϕ_2 being the polymer volume fraction and T_0 the temperature of the 'first' turbidity measurable by eye or with a photocell when the temperature of the solution is changed very slowly, either raised for a LCST or lowered for a UCST. However, the small temperature increment of e.g. 1–2 K just below T_0 , which induces a phase separation, gathers only a small percentage of the polymer present in the solution in the concentrated phase formed. Further phase separation occurs at each subsequent temperature increment. It has been found that complete phase separation for a narrow MW distribution sample does not occur over a few degrees but is spread over a temperature interval which varies with the polymer–solvent system. In the two solvents chosen for the MW characterization in this work, namely *n*-pentane and 2-methylbutane, the interval of observable phase separation spread over as much as 40 K ($M_w = 135\,000$). This interval is observable easily when the temperature is raised by steps, the turbidity generated in the solution at the onset of phase separation being a

very sensitive detector of the formation of a new phase even when the amount of polymer involved is small.

Measurement of turbidity during phase separation: the thermogram

At the LCST, a concentrated phase in equilibrium with a dilute phase is formed. The higher MW s distributed in both phases are, however, present in greater concentration in the concentrated phase, as analysis of fractions has indicated. If the temperature is further raised, lower and lower MW s enter in the concentrated phase. The end of the thermogram marks the temperature T_f at which a step of temperature no longer generates a measurable turbidity. The thermogram is the trace of the transient turbidity during phase separation when the temperature is raised by steps between T_0 and T_f , as presented in Figure 1. The transient character of the turbidity is due to the fact that the spontaneous sedimentation due to gravity of the concentrated phase at the bottom of the tube restores the transparency of the solution to its value before the formation of the concentrated phase. In non-polar volatile alkanes used as solvents, the concentrated phase is heavier than the dilute phase.

Determination of MWD through analysis of turbidity has been extensively studied at a phase separation at low temperature (UCST). The conditions necessary to obtain quantitative information have been analysed at an UCST¹⁹ and recently at a LCST^{15–18}. The advantages of the measurements at a LCST lie in the use only of the temperature rather than of a bad solvent to increase the χ parameter and in the rapidity of the phase equilibrium and sedimentation at high temperature. In the turbidimetric titration at a UCST, phase separation is slow so that the cumulative turbidity for all the successive phases generated by the addition of the non-solvent was measured, instead of the individual turbidity for each phase as recorded in Figure 1.

In the second part of the present work, only the T_0 were measured and the values compared for the series of solvents. In these experiments, the solutions were not heated by increment but submitted to a constant temperature ramp ($0.8^\circ\text{C min}^{-1}$). Since in this part of the paper, we are interested in the comparison of the LCST and not in MWD, knowledge of T_0 only is satisfactory.

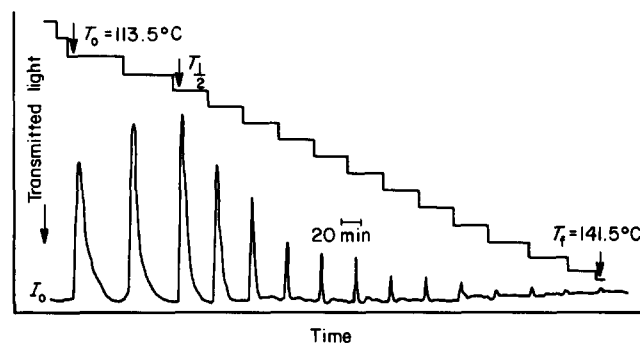


Figure 1 Thermogram of a solution of a narrow MWD *cis*-PIP sample in *n*-pentane; $M_w = 460\,000$ ($M_w/M_n = 1.04$), $\phi_2 = 0.02$, rate of temperature increase 0.8 K min^{-1} . With the temperature program used ($\Delta T = 2\text{ K}$) the thermogram consists of 15 peaks between $T_0 = 113.5^\circ\text{C}$ and $T_f = 141.5^\circ\text{C}$. The temperature at which half the turbidity has been evolved, $T_{1/2}$, is 117.5°C . The stair-like graph above the thermogram is the recording of the temperature program

EXPERIMENTAL

Solvents. These were purchased from the Aldrich Co. (Milwaukee, WI) or the Chemical Sample Company (Columbus, OH) and used without purification. Their physicochemical data (density, expansion coefficient, critical temperature) needed for the calculations are listed in Reference 7. The density measured with a Picker densitometer is used as a control of the solvent quality.

Polymers. For the *MW* characterization analysis in *n*-pentane and 2-methylbutane the polymers used were five atactic narrow MWD samples of polyisoprene bought at the Polymer Laboratories (Massachusetts) and analysed by gel permeation chromatography (g.p.c.) by the company. For the thermodynamic analysis (in the second part of the paper) in the alkane series the polymers used were two samples with a medium MWD, a *cis*- and a *trans*-PIP bought from the SP² Company (Ontario, NY). Their molecular weights measured by intrinsic viscosity have been found to be 180 000 for the *trans* sample and 780 000 for the *cis* sample.

Apparatus. A small oven whose temperature is monitored by means of a temperature programmer TGC85 (Setaram, France) has a isothermal temperature stability of 0.1–0.2°C. The polymer volume fraction, ϕ_2 is usually 0.02 or 0.03 for the characterization and between 0.008 and 0.04 for the determination of the cloud-point curves (CPC) in the thermodynamic analysis.

To obtain a quantitative analysis of the turbidity during phase separation, the following simple set-up was devised. A sealed glass tube containing 0.6 cm³ of the solution ($0.008 < \phi_2 < 0.03$) is placed in the oven. A beam of light is recorded on a photocell after passing through the upper part of the solution. A double channel recorder is used to register simultaneously the signals from a thermocouple and the photocell. The scattering of light is caused by the heterogeneous system constituted by the droplets of concentrated phase in the dilute phase. Before sedimentation, the scattered intensity diminishes, due to the growth in size of the droplets. It has been found by experience that the height of the turbidity peak which develops within minutes after the temperature step is a more reliable indicator of the amount of polymer phase separating than its area, a result similar to that obtained at a UCST²⁰. The duration of a thermogram is of the order of 5–7 h, while the simple determination of T_0 takes <1 h once the solution is well dissolved. When the temperature is raised at a constant rate, the thermogram looks like a differential scanning calorimetry (d.s.c.) melting curve starting at T_0 . This technique has been very useful in analysing semi-quantitatively mixtures of industrial polymers such as the PE–PP ‘block’ copolymers²¹, each polymer appearing as a different curve in the turbidity–temperature trace. However, quantitative analysis either of the respective amounts of the different species or of their polydispersity could not be done in routine conditions due to the lack of equilibrium between turbidity and temperature in this mode of heating.

Quantitative analysis of the data

The assumptions on which rests a quantitative measurement of the MWD include:

(1) A relationship between the temperature of phase separation T_i , and the average *MW*, M_i , of the polymer phase-separating at that temperature. The following

equation is a reasonable relation verified in a similar form at the UCST:

$$T_i = T_\infty + BM_i^{-1/2} \quad (1)$$

where T_∞ is the temperature of phase separation for an infinite *MW* and B a constant which is larger in volatile solvents.

(2) A relationship between the turbidity h_i and amount, m_i , of polymer phase-separating. In a previous work the simple relation

$$m_i = kh_i \quad (2)$$

was used, where k is a constant. A résumé of the justification for equation (2) is given in the Appendix.

Cumulative curve. If k is constant over the temperature range of the thermogram, the normalized turbidity $h_i/\sum h_i = h_i^*$ represents the fraction of the whole polymer which has phase separated at T_i . A plot of h_i^* against temperature gives a quantitative measurement of the fraction of polymer displaced to the concentrated phase as a function of the temperature. $\sum h_i$ is the sum of the turbidity peaks between T_0 and T_f .

With the same assumption concerning k , the molecular weights M_w and M_n are only a function of the set of h_i , T_i and of T and B :

$$M_n = \sum (h_i^*/M_i)^{-1}, \quad M_w = \sum h_i^* M_i \quad (3)$$

The distribution curve obtained by differentiating the cumulative curve in relation to the *MW* can be written as:

$$W(\log M) = d(\sum h_i^{**})/d(\log M) \\ = h_i^* \{ \log[M_i(T_i)] - \log M_i[T_i - \Delta T_i] \} \quad (4)$$

where ΔT_i is the temperature increment which gives rise to the turbidity h_i , and h_i^{**} is the cumulative normalized turbidity. The expression

$$W(\log M_i) = h_i^* \{ 2 \log[1 + \Delta T_i/(T_i - T_\infty)] \}^{-1} \quad (5)$$

obtained after rearrangement, shows that the right-hand side of equation (5) does not depend on B explicitly. However, the left-hand side of (5) uses the two constants of equation (1) to convert T_i in M_i .

The justification of equation (2) by experimental measurement has been presented in Reference 15. The more refined equation

$$m_i = k'h_i^{3/2} \quad (6)$$

can be justified¹⁷ on theoretical grounds. The effect of using equation (2) or equation (6) on the calculated M_w and M_w/M_n will be noted below.

Free volume theory of polymer solutions

The relationship between T_i and M_i in equation (1) is a very convenient way to relate molecular size and phase separation temperature. It has been justified by many experimental data on cloud-point curves at the UCST and LCST. However, as mentioned in the Introduction, systems with a narrow solubility gap have a large *MW* dependence of T_i and the relationship between T_i and $M_i^{-1/2}$ is not linear. A more accurate description of the relationship must be looked for in the free volume theories of polymer solutions, which will be described only succinctly below because detailed accounts can be found in the literature^{2–6,8–13}. The conditions for phase separation are obtained when $\chi(T)$ found from the free

volume theory is equal to the expression for χ given by the lattice model at the phase separation temperature:

$$\frac{1}{2}(1+r^{-1/2})^2 = c_1 v^2 f(v) + c_1 \tau^2 f'(v) \quad (7)$$

$f(v)$ and $f'(v)$ are functions of one parameter, \tilde{v} , the reduced volume of the solvent only; $c_1 v^2$ and $c_1 \tau^2$ are temperature-independent parameters which characterize, respectively, chemical and free volume differences between solvent and polymer. If the effects of extremities are neglected, these two parameters are independent of MW . The reduced volume at a cloud-point curve (CPC) obtained from equation (7) can be converted into temperature by the equation:

$$\tilde{T} = T^* \tilde{v}^{-1} (1 - \tilde{v}^{-1/3})$$

written with the van der Waals model for the energy; $T = T^* \times \tilde{T}$, where T^* is a reducing parameter for the temperature. Some details of the calculations are given in the Appendix.

RESULTS AND DISCUSSION

(1) Characterization of molecular weight distribution

The two solvents n-pentane and 2-methylbutane were chosen as suitable for offering a narrow solubility gap for PIP because they are volatile at room temperature and also because their 'chemical' term in the χ parameter could be expected to be large. Indeed, a similar polymer, *cis*-polybutadiene was found either to be insoluble in volatile alkanes or to have UCSTs around room temperature¹⁴. The present PIP samples have UCST between -10 and -30°C ¹⁸. As indicated by the values of LCST in e.g. n-heptane, the order of the UCSTs in the same solvent is expected to be, *cis*-PIP, *trans*-PIP, *trans*-PBD and *cis*-PBD, the *cis*-PBD having the narrower solubility interval between UCST and LCST in the solvents where the LCSTs are measurable.

Cumulative turbidity curves. In Figure 2, the data $h^*(T_i)$ of the thermogram in n-pentane for the sample with $M_w = 590\,000$ are plotted cumulatively versus T_i . Each point corresponds to a turbidity peak and one can see that the thermogram of this sample is comparable with that given in Figure 1 but displaced towards lower temperatures. The three characteristic temperatures, T_0 , the temperature of the start of the first turbidity, $T_{1/2}$, the temperature at which half of the total turbidity has

been obtained, and T_f , the temperature of the end of the thermogram have been noted on the cumulative curve and for all the samples in Table 1. The values of T_0 , $T_{1/2}$, $T_{1/2} - T_0$ and $T_f - T_0$ increase when the polymer MW decreases. Similar cumulative turbidity curves are found for the five standards. The large temperature interval (16–40 K) over which these narrow MW distribution samples phase-separate is noteworthy. The value of T_f , which can vary by 2–6°C depending on the last peak counted, does not influence $\sum h_i$ or $T_{1/2}$, due to the low intensity of the last few h_i s.

Linearization of the data according to equation (1). Due to the large range of temperature during which phase

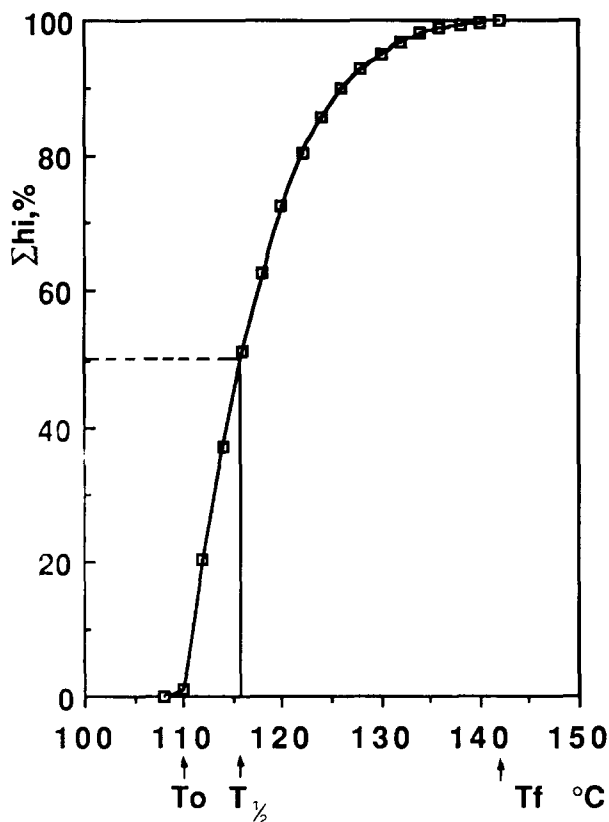


Figure 2 Cumulative curve for another standard ($M_w = 590\,000$, $M_w/M_n = 1.04$) in n-pentane. Each point on the graph corresponds to a turbidity peak. The 15 peaks have evolved between T_0 (110°C) and T_f (142°C). $T_{1/2} = 116^\circ\text{C}$

Table 1 Characterization of *cis*-polyisoprene standards in n-pentane

Solution in n-pentane	G.p.c. analysis	LCST analysis													
		Thermograms						Calculations							
		Characteristic temperatures ($^\circ\text{C}$)						Using equation (1) ^a with				Using equation (7) ^b with			
		Equation (2)	Equation (6)	Equation (2)	Equation (6)	Equation (2)	Equation (6)								
Sample	$10^3 M_w$	M_w/M_n	T_0	$T_{1/2}$	$T_{1/2} - T_0$	$T_f - T_0$	$10^3 M_w$	M_w/M_n	$10^3 M_w$	M_w/M_n	$10^3 M_w$	M_w/M_n	$10^3 M_w$	M_w/M_n	
PIP 135	135	1.04	122	132.5	10.5	40	144	1.25	151	1.20	166	1.27	148	1.20	
PIP 290	290	1.04	116	123.5	7.5	29	256	1.16	259	1.12	294	1.15	253	1.10	
PIP 460	460	1.04	113.5	117.5	4	28	429	1.27	468	1.18	481	1.25	444	1.16	
PIP 590	590	1.06	110	116	6	32	515	1.49	587	1.34	566	1.44	546	1.3	
PIP 1600	1600	1.08	106	108	2	16	1690	1.60	1960	1.49	1601	1.44	1535	1.3	

^a $T_0 = 99.0$, $B = 12\,565$

^b $c_1 \tau^2 = 0.21$, $c_1 v^2 = 0.003$, $T^* = 5960$

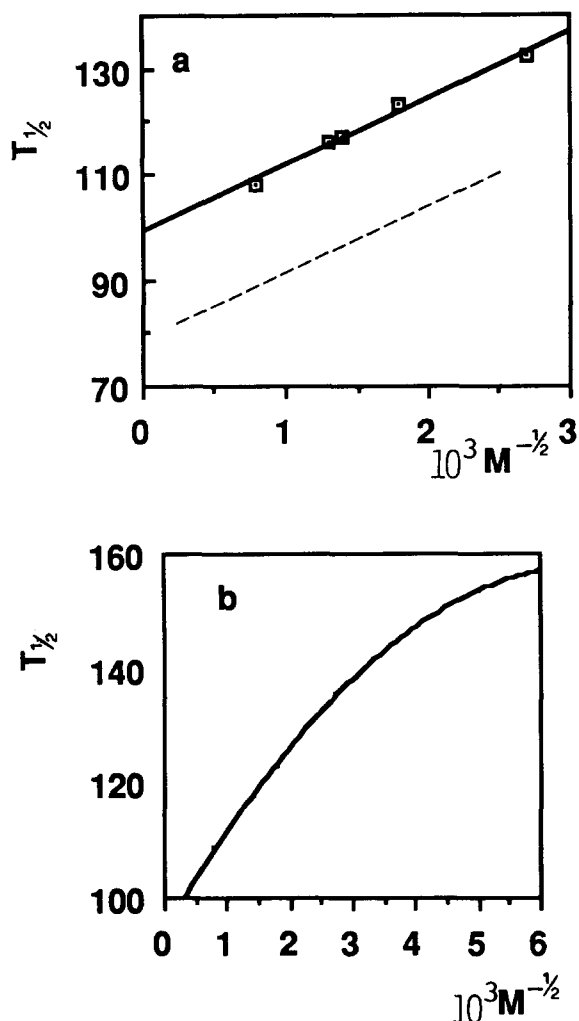


Figure 3 (a) Molecular weight dependence of the characteristic temperature, $T_{1/2}$, read on the n-pentane thermograms for 5 high MW samples. The coordinates are reported in *Table 1*. Linear regression gives $T_{\infty}=99.0^{\circ}\text{C}$ and $B=12\,565$. ---, in 2-methylbutane. (b) Curve fitted with the following values of the parameters in equation (7): $c_1\tau^2=0.21$, $c_1\nu^2=0.003$, $T^*=5958\text{ K}$. The parameters have been chosen to coincide with the experimental LCST for high and lower MW in n-pentane

separation occurs, $T_{1/2}$ should describe a sample more accurately than T_0 . In consequence, the parameters of equation (1) are obtained by plotting, in *Figure 3a*, $T_{1/2}$ versus $M^{-1/2}$ for the five samples in n-pentane. The linearization gives $T_{\infty}=99.0^{\circ}\text{C}$ and $B=12\,565$ for n-pentane and T_{∞} approximately 20 K lower with similar B for 2-methylbutane. The M_w and M_w/M_n calculated by using these constants in equation 2 are given in *Table 1*.

Relationship between turbidity and amount of polymer phase-separating. The results for M_w are satisfactory but the values of polydispersity are too large, particularly for the high MW . A reason for this result was sought in the relationship between the attenuation of the light transmitted, h_i , and the amount of polymer phase-separating. Considering that the photocell detects the light over a solid angle around the beam of incident light, theoretical analysis of the measured quantity¹⁷ led to the relationship given by equation (6). Since this equation gives more weight to high intensity peaks, the resulting effect will be to diminish the polydispersity. As seen in *Table 1*, M_w increases and polydispersity decreases a little

(1.60 to 1.49) for the highest MW . $W(\log M)$ calculated from equations (4) and (6) is given for $M_w=460\,000$ in *Figure 4*.

Use of the equation of state model. Equation (1) has been tested over a narrow MW interval, namely $0.135 < 10^{-6}M_w < 1.6$ and found to reproduce reasonably well the data indicated in *Table 1*. The B values (12 565 and a similar value in 2-methylbutane) are large compared with the value obtained previously, for instance for the system PE + 2,4-dimethylpentane (5200). This is partly because the present solvents are more volatile than 2,4-dimethylpentane and partly because of the narrow solubility gap effect noted in other works⁸⁻¹⁴. To cover a larger domain of MW , a nonlinear relationship between T_i and M_i has to be used, following equation (7). The $T_i(M_i^{-1/2})$ values are plotted in *Figure 3b* and the results for the standards given in the last two columns of *Table 1*. A few measurements of the LCSTs of smaller MW samples indicate that *Figure 3b* gives a good prediction of the experimental data. Some information about the parameters ($c_1\tau^2$, $c_1\nu^2$ and T^*) is given in the Appendix.

Evaluation of polydispersity. The diminution of the polydispersity (from 1.49 to 1.3 for the highest MW) reported in the last column of *Table 1*, brought about by the use of equation (7), comes from the fact that the curvature of the $T_i(M_i^{-1/2})$ curve reduces the range of MW associated with a given range of T_i . The polydispersity, however, is still higher than measured by g.p.c. It is possible to lower M_w/M_n by increasing the curvature of the $T_i(M_i^{-1/2})$ curve through a shift of constants. However, since physical effects can contribute

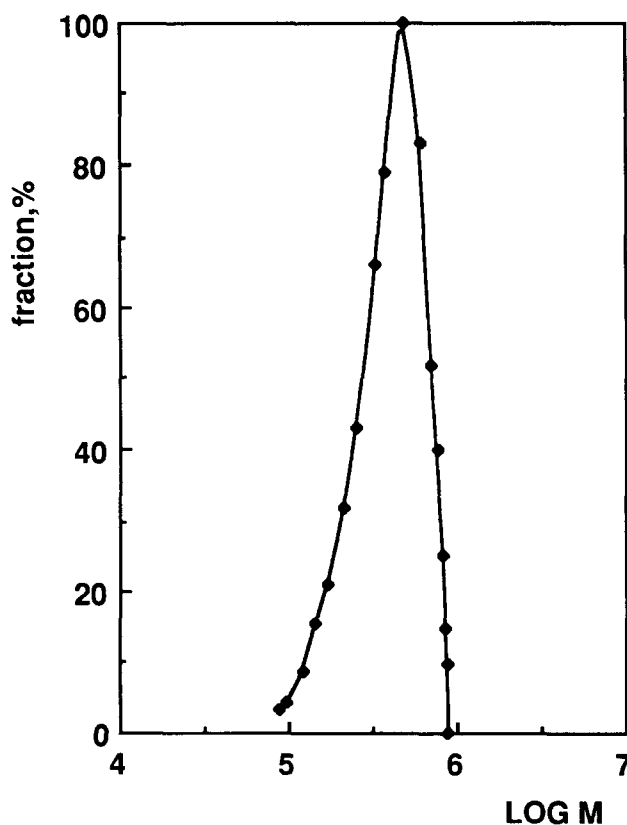


Figure 4 Molecular weight distribution function of sample with $M_w=460\,000$ calculated using equations (6) and (7)

to give different values to M_w/M_n in the LCST and g.p.c. methods, it was not thought worthwhile to report these calculations.

Looking at the last peaks of the thermogram in Figure 1, one notes the sensitivity of the method in detecting small amounts of lower MW . An advantage of this incremental method of fractionation is to gather all the MW s due to phase-separate over the temperature interval ΔT_i . Particularly at high temperature, where a given ΔT_i covers a much smaller range of MW , the size of the temperature increment may be increased up to 5 K. In this manner, it is likely that small amounts, lost in the baseline of the g.p.c. trace, are detectable with the present technique. However, deleting a few peaks at high temperature will not reduce the polydispersity sufficiently. On the other hand, polydispersity is very sensitive to the low temperature, high MW peaks. It is difficult to foresee how the present large peaks could be changed. If the first temperature increments are put to 0.5 or 1°C, it would perhaps be possible to have a small peak develop below that at 113.5°C in Figure 1. But this split of the first peak would increase the polydispersity. On the other hand, it is possible that the same fraction of high MW is just at the limit of detection in the g.p.c. baseline, which follows continuous changes in the solution concentration. Analysis of the assumptions made in the high MW calibration and of g.p.c. data obtained with a more concentrated solution in collaboration with g.p.c. specialists may help us to understand the origin of this difference in polydispersity found by the two methods.

Quality of the dissolution. The measurement of turbidity at a LCST is a sensitive way of detecting the presence of aggregates in solution: when aggregates are left in the solution, the nascent concentrated phase adsorbs on them and gives a large turbidity signal. A less dramatic effect occurs when the small MW s are washed over at low temperature with the high MW . This effect gives a steep cumulative curve and a thermogram without turbidity peaks at high temperature. A longer dissolution time with gentle stirring or the use of a less concentrated solution allows the elimination of these artefacts. Compared with other crystalline or non-crystalline polymers, *cis*-PIP seems to form in pentane solutions molecularly well dissolved and free from aggregates. This essential feature of the measurements leads to reproducible results and the absence of large peaks at low temperature. As an example of the quality of the data, a cumulative curve is given in Figure 5 (curve 3) for two different concentrations. One cannot see any difference between the points for the 2 and 3% solutions although the MW is high (460 000).

In 2-methylpentane, which gives solutions near their LCST at dissolution at room temperature, an adequate dissolution requires a longer time. The presence of aggregates in the 2-methylpentane solution of the same sample can be detected from the cumulative curve as seen in Figure 5 (curve 1). The plateau in the high temperature part of the curve which would lead to a double distribution is due to incomplete dissolution. A longer dissolution time leads to the normal cumulative curve 2, and a higher T_0 . Indication of aggregates is also given by the difference between T_0 and $T_{1/2}$, which increases from 1–2°C in an aggregated solution to the normal 3–10°C (according to the MW) in a well dissolved solution. Values obtained for the second and third run

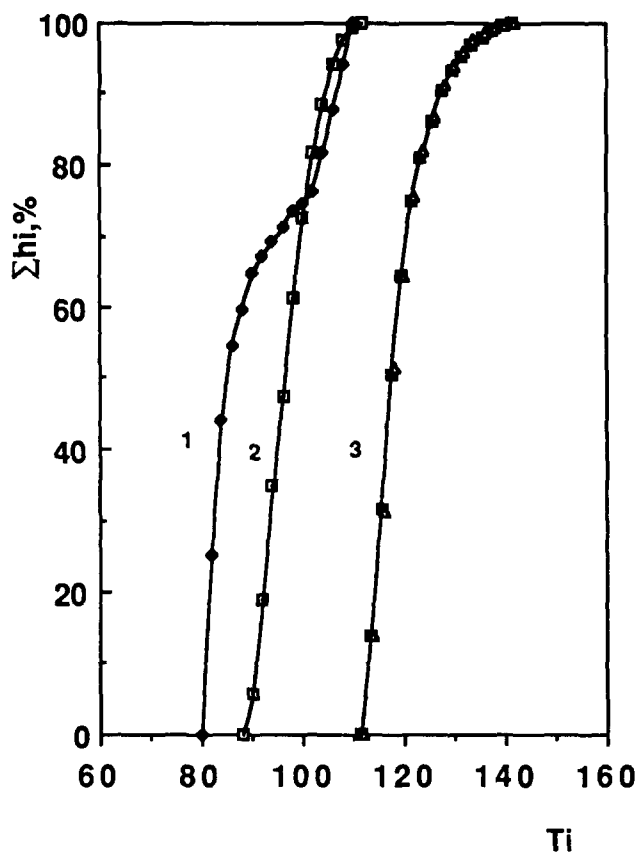


Figure 5 Reproducibility and effect of quality of dissolution as seen on the cumulative curve. Curves 1 and 2, data for the same sample in 2-methylbutane; in the second run (curve 2), the aggregates distorting the shape of curve 1 have disappeared. Curve 3, the data, in *n*-pentane, for the 2 and 3% solutions overlap ($M_w = 460\,000$)

show that no extensive degradation occurs in these oxygen-free solutions during the thermal treatment.

The method of characterization at the LCST described on the *cis*-PIP standards has shown that it gives an alternative to the g.p.c. method with a good description of the MW distribution even in samples of very high MW if an adequate solvent is chosen for the characterization. On the other hand, the sensitivity of the solution properties to polymer stereoregularity, as will be shown in the second part of the paper, could also be used to obtain information on the stereoregularity and the MW distribution of a sample not as uniformly stereoregular as are the standards used. These results give confidence that the method can be adapted to industrial polymers such as rubbers and modified rubbers¹⁶. A low cost method of characterization such as that described above could have a place among the methods of polymer characterization.

(2) Thermodynamic analysis of the LCST of *cis*- and *trans*-PIP in a series of solvents

LCST in polyolefins

Since the molecular origin of the LCST resides in the difference between the degree of expansion of the solvent and of the polymer, one can expect the values of the LCST of a series of non-polar polymers in the same solvent to correlate with their equation of state parameters such as the density or expansion coefficient. This correlation was indeed verified on a series of polyolefins (polypropylene (PP), polyisobutylene, polybutene, polybutene, poly-4-methylpentene)⁷ in a series of solvents, mainly alkanes. However, polyethylene (PE)

was found to be an exception with unexpectedly low LCSTs. For instance, in 2,4-dimethylpentane, a good solvent for PE and crystalline PP, the LCSTs are respectively 134 and 200°C for an infinite MW . In the systems studied, the 'chemical contribution' coming into the χ parameter between 130 and 200°C is unlikely to be larger for PE than for PP. The origin of the higher χ parameter or of the low LCST must be related to a structural contribution which arises at the dissolution in the case of PE and is minimal for PP. Correlations of molecular orientations (CMO) in the melt, no longer able to form in the dilute solution, provide the extra contribution to χ . In other words, a low LCST is thermodynamically favoured since in the concentrated phase which forms, a fraction of the CMO present in the melt is restored. Information on PE solutions at high temperature given by data such as A and B is relevant to the understanding of another change of phase, namely the crystallization out of solution. Recent work^{27,28} stresses the importance of the nature of the solvent and other factors (temperature, molecular weight) on the competition at high temperature between the two modes of crystallization, which leads either to the chain-folded crystals or the shish-kebabs. Similarly, better understanding of the solution behaviour near the LCST of non-crystallizable polymers (or of polymers crystallizable at low temperature, such as the rubbers) is likely to shed some light on the problems of gel and aggregates common in some solvents. The following analysis of LCSTs of PIPs of different stereoregularity has been done in this context.

The PIP standards have remarkably low LCST values in the two volatile solvents used for the characterization, namely n-pentane and 2-methylbutane. The low expansibility of a polymer at the origin of the LCST is easily measurable by its expansion coefficient, a low expansion coefficient leading to a low LCST. The temperatures of phase separation are as low for PIP as they are for polyisobutylene (PIB) in the same solvents although the expansion coefficient of PIP alone, which at $0.70 \times 10^{-3} \text{ K}^{-1}$ is much higher than that of PIB ($0.55 \times 10^{-3} \text{ K}^{-1}$), would predict considerably higher LCST. Clearly, another important contribution must increase the χ parameter.

To confirm the hypothesis of the importance of segment shape on the thermodynamics of solutions at high temperature and in particular on the LCST, systematic measurements of phase separation of two

stereo-isomers of PIP (a *cis* and a *trans* sample) were made in a series of solvents and are reported below.

Cloud point curves of *cis*- and *trans*-PIP in the linear and branched alkane series

The T_0 values at the minimum of the cloud-point curves (CPC) were measured in a series of linear and branched alkanes for two polydisperse polyisoprenes, a *cis* and a *trans* sample. The results are reported in Figure 6 and the data are listed in the Appendix. Only two CPC are given in Figure 6a, those obtained in n-heptane for the two isomers, but similar curves are found for the other solvents.

Comparison of *cis*- and *trans*-PIP and data in linear and branched alkanes

The trend of the LCSTs and, in particular, the importance of the free volume term can be assessed by correlating T_0 with a parameter characteristic of the volatility of the solvent such as the expansion coefficient. For solvents which are chemically similar, the density at 25°C is a simple measurement of the solvent expansion at 25°C, so it is used as the correlating parameter in Figure 6b for the linear alkanes and in Figure 6c for the branched alkanes. The open symbols are for *trans*- and the closed ones for the *cis*-PIP. When the data for each isomer are joined by a line (Figures 6b and c), one can see that the T_0 s in the different solvents are lower for the *trans*-isomer (by about 25°C at low temperature) than for the *cis*-isomer, but this effect diminishes at high temperature since, in nonane, the T_0 for *cis*- and *trans*-PIP are effectively the same. Also, if a linear and a branched solvent with the same density are compared, the linear solvents have LCSTs higher (by about 30 K) or give a better solution than branched isomers. Cowie *et al.*¹³ noted also that in aromatic solutions, where the LCSTs are high due to the strong cohesive energy of the solvent, the *cis*- and *trans*-isomers had very similar LCSTs. The data for the two isomers have been compared irrespective of their different MW because, if a correction were made, it would increase the gap between the *cis* and the *trans* samples.

It seems justified to associate the low LCSTs for PIP and the lower values in the *trans* sample with the presence of CMO between the polymer chains in the concentrated phase, as in PE. If the *trans*-isomer, due to its regular segment shape, can more easily make CMO in solution, the concentrated phase where CMO are more probable

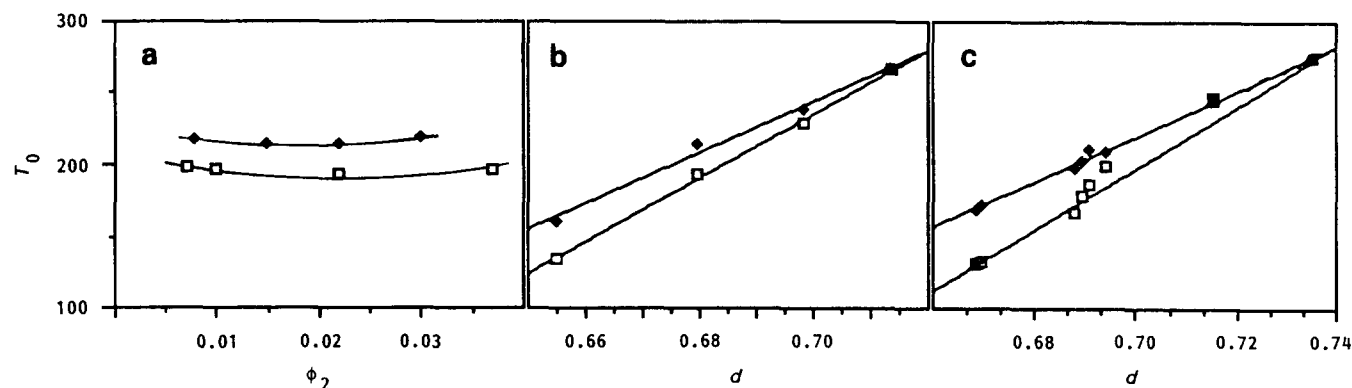


Figure 6 Minima of the cloud-point curves for two polydispersed samples of *cis*- and *trans*-PIP in a series of linear and branched alkanes. (a) Cloud-point curves depicting the temperature of first turbidity versus ϕ_2 , the polymer volume fraction, in one solvent, heptane, for *cis*- (\blacklozenge) and *trans*-PIP (\square). (b), (c), minima of the cloud-point curves, T_0 , for *cis*- (\blacklozenge) and *trans*-PIP (\square) against solvent density at 25°C for the linear alkanes, (b), and the branched alkanes, (c)

will be stabilized and consequently form at a lower temperature than in the *cis*-isomer. While the presence of a methyl group every second carbon in PP was sufficient to reduce molecular contacts leading to CMO, the presence of a methyl side group every four carbons situated near a double bond may well give the right combination of flexibility and restrained mobility to favour CMO. The greater ease that the linear alkanes now have of creating some form of CMO between the solvent and the polymer may be invoked also to explain the much higher values of the LCST for the linear alkanes (about 30 K) in volatile solvents. There is no contradiction between the two previous arguments since CMO between the polymer chains are favoured by a concentrated phase, while some energetically favourable shape-related solvent-polymer contact interaction occurs in the dilute phase. Similar variation at room temperature of the χ parameter according to the matching of segment and solvent shape has been found by intrinsic viscosity²⁵ and calorimetric analysis²⁶ on a variety of atactic polymers and at higher temperature^{19,24} on PE and random ethylene-propylene copolymers.

To illustrate the contrast between PE and the other polyolefins, the experimental LCST, reduced by the solvent critical temperature T_c , i.e. $LCST/T_c$, have been plotted *versus* the free volume term^{7,23} $c_1\tau^2$ as in Figure 7. The parameters $c_1\tau^2$ are calculated simply from the experimental coefficient of expansion of these polymers

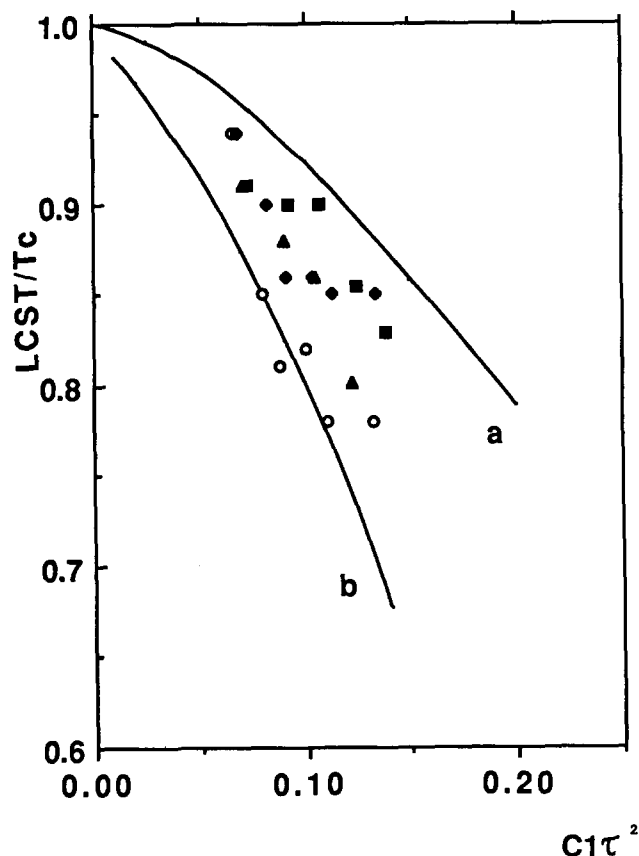


Figure 7 Comparison of LCSTs for *cis*- and *trans*-PIP with those of other polyolefins in a series of alkanes. The reduced LCSTs, $LCST/T_c$ (where T_c is the solvent critical temperature), are plotted against a parameter characteristic of the free volume term, $c_1\tau^2$. Curve a is for several polyolefins (PIB, PP, P4MP), curve b is for PE; points between are for *cis*- (■, ◆) and *trans*-PIP (▲, ○). The overall positions of the PIP LCSTs, particularly those of the *trans* values, support the assumption of CMO in melt PIP, as in PE

as detailed in the Appendix. Curve a runs through the data (not reported individually here but given in Reference 7) in about 20 solvents for four polyolefins and curve b corresponds to the values for linear PE in the same solvents. The points between the curves are for PIP (including the two values for one of the standards obtained in the first part of this paper). From the remarkable difference between curves a and b (and other considerations related to the thermodynamics of small-molecule mixtures) the hypothesis of CMO as agents for lowering the LCST was advanced. Those CMO are predicted to be stable until a temperature which depends on the free volume of the system and would be $\approx 170^\circ\text{C}$ for melt PE⁷. The positions of the points in the $LCST/T_c(c_1\tau^2)$ graph suggest a similarity between PE and PIP, particularly the *trans*-isomer. A certain amount of order among the chains in the melt below 100°C is not unlikely because the range of melting temperatures of both isomers is not too far below the LCST.

The overall thermodynamic effect of CMO in the melt is to give a positive contribution to the χ parameter in equation (7) and to lower the LCST. There was no obvious alternative to the origin of this effect, for PE, because the negligible chemical difference between PE and the alkanes could not contribute to lower substantially the χ parameter (first term in equation (7)). One can wonder if the same reasoning is as strong with PIP since the regularly placed double bonds must raise the chemical difference between the alkanes and the polymer, with the effect of displacing curve a towards the experimental points for PIP. To obtain an answer to that question, some values of heats of mixing will be recalled. The heats of mixing of two liquids A and B are a very sensitive indicator of chemical difference between the groups of atoms constituting A and B. The successful use of model molecules to predict polymer compatibility indicates that heats of mixing of liquids can give valuable information on polymer-solvent mixtures. As examples of the order of magnitude of the heats of mixing in J mol^{-1} at the middle of the concentration range, one can quote two extremes: a branched alkane mixed with another branched alkane gives a heat of about 50, while if the same alkane is mixed with a polar compound, trifluoroethanol¹⁸, the result is 1500. Heats of mixing²⁶ of a branched alkane with another alkane containing one oxygen atom, dioctylether (I), or a double bond 5-decene (II) are, respectively, 150 and 18 (actually 35 for the *cis*- and 11 for the *trans*-5-decene). Since the value of (II) which contains a double bond is very low, similar to the value which would be obtained for the mixture of two branched alkanes, one can conclude safely that the chemical term associated with the formation of a contact between an aliphatic segment and a segment containing a double bond is really small, smaller than if the segment includes an oxygen atom. Consequently, the origin of the low LCSTs for PIP must be something other than a chemical term. The similarity in Figure 7 between the displacement of $LCST/T_c$ for PIP (points) and PE (curve b) supports the presence of CMO in the concentrated phase or in the melt of PIP.

The present work constitutes a different approach to the study of order in the melt or in the amorphous phase, order which has been investigated by various methods. Change of order or of chain mobility has been seen when the temperature increases, by using techniques including d.s.c. analysis, Brillouin scattering and thermostimulated

current. Confirmation of the present analysis in solution on PIP may come from these methods applied in the solid state.

ACKNOWLEDGEMENT

The support of the National Science and Engineering Research Council of Canada is gratefully acknowledged.

REFERENCES

- 1 Freeman, P. I. and Rowlinson, J. S. *Polymer* 1960, **1**, 20
- 2 Delmas, G., Patterson, D. and Somcynsky, T. *J. Polym. Sci.* 1962, **57**, 59
- 3 Patterson, D. and Delmas, G. *Trans. Faraday Soc.* 1969, **65**, 708
- 4 Patterson, D. and Delmas, G. *Discuss. Faraday Soc.* 1979, **49**, 98
- 5 Patterson, D. and Delmas, G. *Int. Symp. Macromol. Chem.*, Toronto, 1968
- 6 Eichinger, B. E. and Flory, P. J. *Trans. Faraday Soc.* 1969, **64**, 2035
- 7 Charlet, G. and Delmas, G. *Polymer* 1981, **22**, 1181
- 8 Siow, K. S., Delmas, G. and Patterson, D. *Macromolecules* 1972, **5**, 29
- 9 Saeki, S., Konno, S., Kuwahara, N., Nkata, M. and Kaneko, M. *Macromolecules* 1974, **7**, 521
- 10 Saeki, S., Kuwahara, N., Konno, S. and Kaneko, M. *Macromolecules* 1974, **6**, 246
- 11 Saeki, S., Kuwahara, N., Konno, S. and Kaneko, M. *Macromolecules* 1974, **6**, 589
- 12 Cowie, J. M. G. and McEwen, I. J. *Polymer* 1975, **16**, 244
- 13 Cowie, J. M. G. and McEwen, I. J. *Polymer* 1975, **16**, 933
- 14 Delmas, G. and de St Romain, P. *Eur. Polym. J.* 1974, **10**, 1133
- 15 Barbalata, A., Bohossian, T., Prochazka, K. and Delmas, G. *Macromolecules* 1988, **21**, 3286
- 16 Bohossian, T., Caceres, P. and Delmas, G. *Rubber Rev.* in press
- 17 Bohossian, T., Benoit, H. and Delmas, G. *J. Polym. Sci.* in press
- 18 In this laboratory, unpublished work
- 19 Urvin, J. R. Molecular weight distribution by turbidimetric titration, in Huglin, M. B. 'Light Scattering by Polymer Solutions', Academic Press, London, 1972, p. 789
- 20 Beattie, W. H. and Jung, H. C. *J. Colloid Interface Sci.* 1968, **27**, 581
- 21 Besombes, M., Mengual, J. F. and Delmas, G. *J. Polym. Sci., Polym. Phys. Edn.* 1988, **26**, 1881
- 22 Keinath, S. E., Miller, R. L. and Rieke, J. K. 'Order in the Amorphous State', Plenum Press, New York, 1988
- 23 Charlet, G. and Delmas, G. *Polymer* 1981, **22**, 1190
- 24 Filiatrault, D., Phuong-Nguyen, H. and Delmas, G. *J. Polym. Sci. Polym. Phys. Edn.* 1981, **19**, 771
- 25 Phuong-Nguyen, H. and Delmas, G. *Macromolecules* 1979, **12**, 740
- 26 Delmas, G. and Nguyen Thi Thanh *Trans. Faraday Soc.* 1975, **71**, 1172
- 27 Narth, K. A., Barham, P. J. and Keller, A. *Macromolecules* 1982, **15**, 464
- 28 Phuong-Nguyen, H. and Delmas, G. in preparation

APPENDIX

Justification of the hypothesis

The validity of the equations used in this paper is discussed in detail in Reference 15. We report here the three tests developed to ensure the suitability of equation (2). The first consists of analysing the cumulative turbidities for 11 solutions with ϕ_2 such as $0.018 < \phi_2 < 0.04$. $\sum h_i$ is found to be a linear function of ϕ_2 which extrapolates at the origin. In the second test, each point of a cumulative curve is plotted after normalization for the concentration (h_i/ϕ_2) against T . All the data obtained for different concentrations fall on the same curve. The third test is a correlation of gravimetric

and turbidimetric analysis. Several solutions at the same concentration are prepared and analysed by their thermograms taken from T_0 to a temperature T_i which is different for each tube. The concentrated phase of each solution is characterized by h_i , its cumulative turbidity between T_0 and T_i . After equilibrium at T_i , the polymer in the concentrated phase is then separated and its weight, w_i , determined gravimetrically for each solution. For seven solutions measured over the interval of phase separation, a good correlation is obtained between h_i and w_i .

The absolute value of the signal generated when the concentrated phase forms, i.e. the constant k of equation (2), depends on the rate of temperature increase, v , but the relative values of the h_i s were found to be independent of v (Reference 15). Concentration and temperature increments are adjusted in order not to have too large a value of the attenuation of light. Typically, the $\ln(I_0/I)$ values lie between 0 and 0.5, I_0 being the light transmitted before or between phase separation and I (or h_i) the maximum of the turbidity peak.

Equation of state calculations

Parameters for the solvents and the polymer. The reduced volumes and temperatures can be calculated from the expansion coefficients

$$\tilde{v}^{1/3} = [(4/3)\alpha T + 1]/(\alpha T + 1)$$

and

$$\tilde{T} = \tilde{v}^{-1}(1 - \tilde{v}^{-1/3})$$

in the van der Waals model used by several authors¹⁻¹¹. With $\alpha = 0.68 \times 10^{-3}$ and 1.65×10^{-3} for *cis*-PIP and *n*-pentane, respectively, the values of T^* are found to be 6530 and 4215 K, respectively. The value of $c_1 = P^*V^*/T^*$ is 1.1, as calculated in the literature using for the same model $V^* = V/\tilde{v}$, where V is the molar volume and $P^* = \gamma \tilde{v}^2 T$.

Parameters in equation (7). The two functions $f(\tilde{v}) = (1 - \tilde{v}^{-1/3})^{-1}$, which diminishes when T increases, and $f'(v) = \{2[(4/3)\tilde{v}^{-1/3}]\}^{-1}$, which increases with T , reflect the temperature variations of the two contributions to the parameter (chemical and free volume differences between polymer and solvent) when the temperature increases. Approaching the LCST, the first term becomes negligible compared to the second. Consequently, the normalized LCST, $LCST/T_c$, is for several polymers in many solvents almost exclusively a function of $c_1\tau^2$ (curve a of Figure 7);

$$c_1\tau^2 = (1 - T_1^*/T_2^*)^2 = 0.14$$

for the *cis*-PIP pentane system.

Calculation of the coexistence curve in Figure 3b. In this case, it is no longer the trend of the LCST which is of interest but the exact value and its dependence on MW . The calculated $c_1\tau^2$ used in Figure 7 is now allowed to be changed to overcome the inadequacy of the van der Waals model, which is more apparent at low temperature. To cover the interval of temperature $T_i(M_i)$ found experimentally, $c_1\tau^2$ is increased to 0.21. To reproduce the curvature of $T_i(M_i^{-1/2})$, found when the lower MW s are taken into account (Figure 3b), one has the choice of changing the balance of $c_1\tau^2$ and c_1v^2 or writing arbitrarily that $c_1\tau^2$ is a diminishing function of

MW , namely $c_1 \tau_\infty^2 (1 - Ur^{-1/2})$. In Figure 3b the second method, which gives (with $U = 0.8$) an adequate curvature for $T_i(M_i^{-1/2})$, is reported but other sets of parameters could give similar results. The actual temperature is found by shifting T^* to 5960 for n-pentane.

The term r in equation (7) is taken as the ratio of the molar volumes of the polymer and the solvent. In this part of the phase diagram, where the CPC varies rapidly with MW , an exact fitting is a requirement to obtain a good value of M_w and M_w/M_n from the thermogram and equation (7). The linear equation of Figure 3a covers only the high MW . However, for most of the systems¹⁵⁻¹⁷, equation (1) gives quite a good description of the $T_i(M_i)$ relationship over the range of usual molecular weights.

Numerical data

Thermogram in Figure 1. Peaks of attenuation of light in the thermogram: for a 3% solution in n-pentane with $v = 1 \text{ K min}^{-1}$, a typical set of 15 peaks of T_i ($^\circ\text{C}$), h_i (arbitrary units), for $M_w = 0.46 \times 10^6$, reads as follows: 113.5, 67; 115.5, 85; 117.5, 91; 119.5, 66; 121.5, 51; 123.5, 30.5; 125.5, 23.5; 127.5, 22; 129.5, 13; 131.5, 13; 133.5, 8; 135.5, 4.5; 137.5, 4; 139.5, 2; 141.5, 1.5.

The percentage transmission through the solution during phase separation is obtained from h_i by the

expression $100(1 - h_i/210)$. The diminution of I_0 at high temperature ($\approx 2\%$), which starts at about 133–135 $^\circ\text{C}$ and is due to the rapid expansion of the solvent is not taken into account in the calculations.

Figure 6—temperatures of first turbidity, T_0 , at the minimum of the cloud-point curve. Figure 6a, cloud-point curves in n-heptane: the temperatures are in $^\circ\text{C}$ and the data in parentheses give the polymer volume fraction. *Trans*-PIP: 196 (0.007); 198 (0.01); 194 (0.022); 196 (0.037). *Cis*-PIP: 218 (0.008); 215 (0.015); 215 (0.022); 220 (0.03).

Figures 6b and c. The first two numbers after the name of the compound are T_0 for the *trans*- and *cis*-isomers, respectively, in $^\circ\text{C}$ and the third number, the abscissa of Figures 6b and c, is the solvent density at 25 $^\circ\text{C}$.

Linear alkanes: n-hexane, 134,161,0.6548; n-heptane, 194,215,0.6795; n-octane, 230,239,0.6985; n-nonane, 267,268,0.7138.

Branched alkanes: 2,4-dimethylpentane, 131,169,0.6683; 2,2-dimethylpentane, 132,172,0.6695; 2,2,4-trimethylpentane, 168,198,0.6878; 2,5-dimethylhexane, 178,203,0.6893; 2,3-dimethylpentane, 187,211,0.6909; 3-ethylpentane, 200,210,0.6939; 3,4-dimethylhexane; 248,247,0.7156; 2,2,4,4,-tetramethylpentane, 246,245,0.7156; 2,3,4-trimethylhexane, 275,275,0.7354.